Scientific Research Publishing

Materials Sciences and Applications, 2020, 11, 1-11
https://www.scirp.org/journal/msa
ISSN Online: 2153-1188
ISSN Print: 2153-117X

Anomalous Proton Conductivity in Chitin-Chitosan Mixed Compounds

Takashi Kawabata, Yusuke Takahashi, Yasumitsu Matsuo

Department of Life Science, Faculty of Science & Engineering, Setsunan University, Ikeda-Nakamachi, Neyagawa, Osaka, Japan
Email: t.kawabata_17d_kyousei@outlook.com

How to cite this paper: Kawabata, T., Takahashi, Y. and Matsuo, Y. (2020) Anomalous Proton Conductivity in Chitin-Chitosan Mixed Compounds. *Materials Sciences and Applications*, **11**, 1-11.
https://doi.org/10.4236/msa.2020.111001

Received: November 6, 2019
Accepted: December 28, 2019
Published: December 31, 2019

Abstract

In order to investigate a key factor for the appearance of proton conductivity in chitin-chitosan mixed compounds, the chitin-chitosan mixed compounds $(\text{chitin})_x(\text{chitosan})_{1-x}$ were prepared and these proton conductivities have been investigated. DC proton conductivity σ_0 is obtained from Nyquist plot of impedance measurement data, and the relationship between σ_0 and mixing ratio x has been made clear. It was found that the x dependence of σ_0 is non-monotonous. That is, σ_0 shows the anomalous behavior, and has peaks around $x = 0.4$ and 0.75. This result indicates that there exist optimal conditions for the realization of high-proton conductivity in the chitin-chitosan mixed compound in which the number of acetyl groups is different. From the FT-IR measurement, we have found that the behavior of proton conductivity in $(\text{chitin})_x(\text{chitosan})_{1-x}$ is determined by the amount of water content changed by x. Using these results, proton conductivity, which is important for the application of conducting polymers in chitin-chitosan mixed compounds, will be able to be easily controlled by adjusting the mixing ratio x.

Keywords

Chitin, Chitosan, Mixed Compounds, Proton Conductor, Biomaterial

1. Introduction

Recently, biomaterials have been attracting attention as clean next-generation materials [1] [2] [3]. As well-known, tissue-derived biomaterials are biodegradable and environmentally friendly, and therefore it is expected that tissue-derived materials become new functional materials toward the next-generation. Chitin is one of the tissue-derived biomaterials and is a polymer of N-acetylglucosamine. In addition, chitin is well-known as the main component of shell such as crabs

and shrimps and is abundantly present in nature. Recently, chitin's excellent biocompatibility and strength are widely used not only in the medical field but also in the industrial field. Allan *et al.* reported that chitosan gives the wet strength of paper [4]. Nair and Madhavan have investigated the method for the elimination of Hg in solution using chitosan [5]. Schwarz *et al.* reported the adsorption effect of iron and sulfate ions on chitosan membrane [6]. Leslie *et al.* showed that chitin and chitin derivatives have an effect of promoting wound healing [7]. Nunthanid *et al.* reported the results of using spray-dried chitosan acetate and ethylcellulose as a new compressed coat of 5-aminosalicylic acid tablets [8]. Tripathi *et al.* reported on the preparation and antibacterial activity of chitosan-based films for food packaging [9]. Kim *et al.* reported on the potential of chitosan bio-devices [10]. Kenawi *et al.* Reported that chitosan and its derivatives could be used for medicinal purposes [11]. However, the applications of chitin are few in the energy field. As well known, in recent years, fuel cells have attracted attention as a next-generation energy. The problem with fuel cells is that the cost of the electrolyte is high, and environmental impact is imposed during manufacturing and disposal. Recently, we have fabricated the fuel cell using the electrolyte of chitin or chitosan which is known as the deacetylated chitin. Chitin and chitosan are available at low cost and are environmentally friendly. **Figure 1(a)** and **Figure 1(b)** respectively show the current-cell voltage characteristics of fuel cell using the chitin electrolyte and chitosan electrolyte obtained by the injections of hydrogen and oxygen fuel gas. It is evident that these current-cell voltage characteristics show typical characteristics of the fuel cell. These results indicate that the chitin and chitosan become the electrolyte of fuel cells. Further, as shown in **Figure 1(a)**, the fuel cell-based on chitin electrolyte operates at maximum power density 1.35 mW/cm^2, while the fuel cell using the chitosan electrolyte shows the maximum power density of 0.032 mW/cm^2 [12] [13]. The prepared fuel cell used platinum electrodes and a 70 μm thick chitin or chitosan sheet as the electrolyte. In this way, the power density of the fuel cell using chitin electrolyte is considerably larger than that using chitosan electrolyte. These results indicate that proton conductivity of chitin is different from

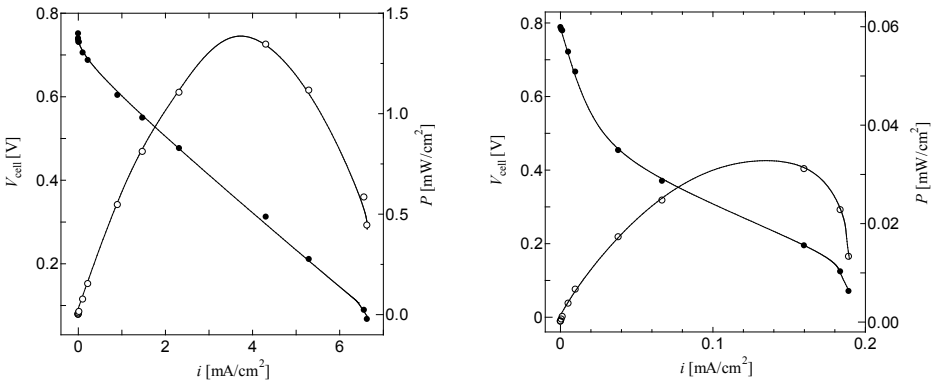

Figure 1. *i-V* characteristics in fuel cells based on chitin electrolyte (a) and chitosan electrolyte (b) [12] [13].

that of chitosan. More recently, we have revealed that chitin becomes superior proton conductor among the natural bio-electrolyte and that the chitin in the humidified condition shows approximately 1.0×10^{-1} S/m, which is approximately 10^3 times higher than that in chitosan [12] [13].

From these facts, it is evident that the acetyl group plays an important role in proton conductivity in chitin system. In addition, it is noted that the open circuit voltage of the fuel cell using the chitosan electrolyte is slightly higher than that using the chitin electrolyte, as shown in **Figure 1(a)** and **Figure 1(b)**. These results indicate that proton conductivity may change by changing the chitin-chitosan mixing ratio. Very recently, we have measured the characteristic feature of proton conductivity in the chitin-chitosan mixed compounds $(\text{chitin})_x(\text{chitosan})_{1-x}$ and obtained the result that the mixing ratio x dependence of proton conductivity shows anomalous behavior. In the present work, in order to clarify the main factor determining proton conductivity in $(\text{chitin})_x(\text{chitosan})_{1-x}$, we have investigated the cause of anomalous behavior of proton conductivity observed in the chitin-chitosan mixed compounds, which is significantly important for fabricating chitin based fuel cell or other electrical devices. The obtained results include the useful information that the properties of biopolymers can be easily controlled by the mixing ratio of polymers. Therefore, the obtained results will be helpful not only to use the fabrication of electrical devices such as field effect transistor or fuel cell based on chitin-chitosan mixed compound but also to fully understand the mechanism of proton conductivity on biopolymers.

2. Experiments

2.1. Preparation of Chitin-Chitosan Mixed Films

The purified chitin 2% (w/v) and chitosan 2% (w/v) were prepared as a slurry of Sugino Machine Ltd. The mixing ratio of chitin and chitosan was adjusted by the weight of chitin. The specimens were formed into films by adding purified water to chitin or chitosan slurry, and suction-filtering using a PTFE membrane filter after sufficient stirring. After 2 to 3 hours of filtration, the specimens were left overnight in a drying oven. These membranes were adjusted to a diameter of 7 cm and a thickness of 0.1 mm for the measurement of proton conductivity. When the mixing ratio is x, the specimens are expressed by the following formula

$$x = W_{\text{chitin}}(\text{g}) \Big/ \left(W_{\text{chitin}}(\text{g}) + W_{\text{chitosan}}(\text{g})\right), \tag{1}$$

where W_{chitin} and W_{chitosan} are the weights of chitin and chitosan, respectively.

2.2. Impedance Measurement

The measurement of electrical conductivity was carried out the range between 100 Hz and 1MHz using precision LCR meter (E4980A, Agilent Technologies Inc.). The relative humidity and fuel gas were controlled by the humidified gas-flow control system of Auto PEM (Toyo Corporation). In the impedance

measurement, proton conductivity parallel to the surface of chitin or chitosan film was measured in the present work.

The proton conductivity was analyzed by Nyquist plot of the measured impedance Z. The impedance Z by the C-R parallel circuit of capacitance C and resistance R is expressed by the following equation,

$$Z = \frac{R}{1+(\omega CR)^2} - j\frac{\omega CR^2}{1+(\omega CR)^2}. \quad (2)$$

Here, ω is angular frequency and j is imaginary unit. The DC proton conductivity in the bulk was derived by extrapolating the circular arc to the real axis for the measured impedance plane.

Here, R and C are resistance and capacitance in the simple C-R parallel equivalent circuit, respectively, and j is imaginary unit.

For $Z' = \frac{R}{1+(\omega CR)^2}$ and $Z'' = \frac{\omega CR^2}{1+(\omega CR)^2}$, the relation between Z' and Z'' becomes the following equation,

$$(Z' - R/2)^2 + Z''^2 = (R/2)^2. \quad (3)$$

In this way, the semicircle part in the impedance plane is caused by the simple C-R parallel equivalent circuit in the specimen. That is, considering these results, the observed semicircle part of Z represents the conductivity and polarization property in bulk of chitin. DC proton conductivity in the bulk of $(\text{chitin})_x(\text{chitosan})_{1-x}$ can be derived by extrapolating the circular arc to the real axis in the impedance plane

2.3. FT-IR Measurement

FT-IR (Fourier Transform Infrared Spectroscopy) was measured using NICOLET iS5 (Thermo Scientific Corp). Chitin, chitosan and mixed samples were prepared as 0.03 mm membranes. The IR measurements were performed between 400 cm^{-1} and 4000 cm^{-1}.

3. Result and Discussion

Figure 2 shows the photograph of the chitin-chitosan mixed membrane of $(\text{chitin})_{0.5}(\text{chitosan})_{0.5}$. Films with other mixing ratios $(\text{chitin})_x(\text{chitosan})_{1-x}$ have the same color appearance, moisture resistance and will not break or melt under humid conditions.

Figure 3 shows the Nyquist plot obtained by the real and imaginary parts of the impedance measurement data for the several mixing ratios around the 80% relative humidity. As shown in Figure 3, in the high frequency region, the relation between the real and imaginary parts of impedance becomes semi-circle arc. Therefore, the obtained results can be described by a parallel equivalent circuit of the components of capacitance C and of resistance R_{DC}. These results indicate that R_{DC} is obtained from intersects of the horizontal axis of semi-circle arc as described above. As seen in Figure 3, R_{DC} of chitin is considerably smaller than

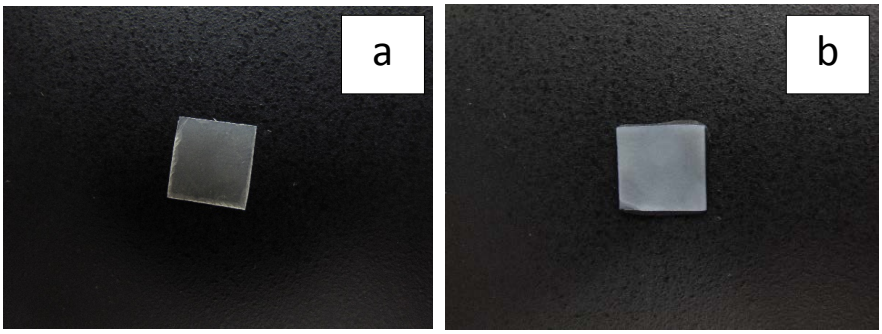

Figure 2. Photograph of dried (a) and wet (b) the mixed membranes of $x = 0.5$.

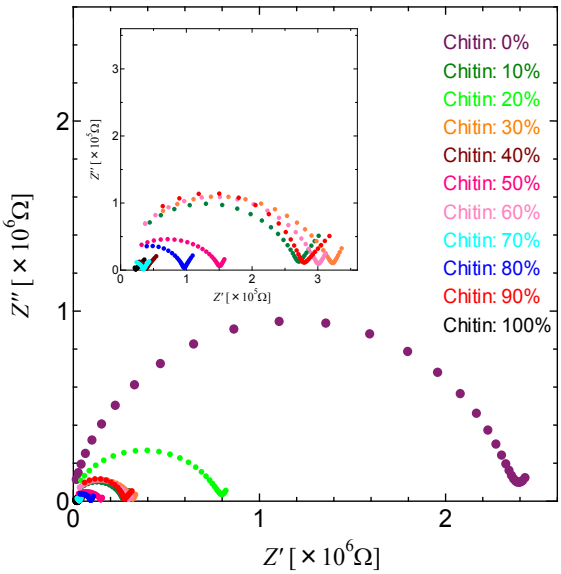

Figure 3. Nyquist plot at 80% humidity in chitin-chitosan mixed compounds. Inset shows the expansion of Nyquist plot below ~3.0×10^5 Ω.

that of chitosan. This result means that proton conductivity in chitin is considerably higher than that in chitosan and therefore is consistent with previous study [10]. Furthermore, we note that the semi-circle arc size doesn't monotonously reduce by the reduction of the mixing ratio *x*. That is, the mixing ratio *x* dependence of R_{DC} isn't monotonous change but shows the anomalous behavior.

The DC conductivity σ_{DC} is obtained from the DC resistance R_{DC}. **Figure 4** shows the relative humidity dependence of σ_{DC} obtained from the analysis of Nyquist plot in **Figure 3**. Here, *x* in **Figure 4** denotes the mixing ratio *x*. The humidity dependence of proton conductivity in each mixing membrane shows a monotonous increase with the increase in relative humidity. In this way, the behavior of the increase in conductivity by increasing R_H is the same in all specimens.

On the other hand, it is noted that the conductivity changes approximately 10 to 100 times by the change of *x*. Moreover, as shown in **Figure 4**, it is evident that proton conductivity shows anomalous behavior with changes of *x*. For example, with increasing *x*, proton conductivity at the 80% relative humidity increases from $x = 0$ to $x \sim 0.4$, but decreases at $x \sim 0.6$ and increases again with

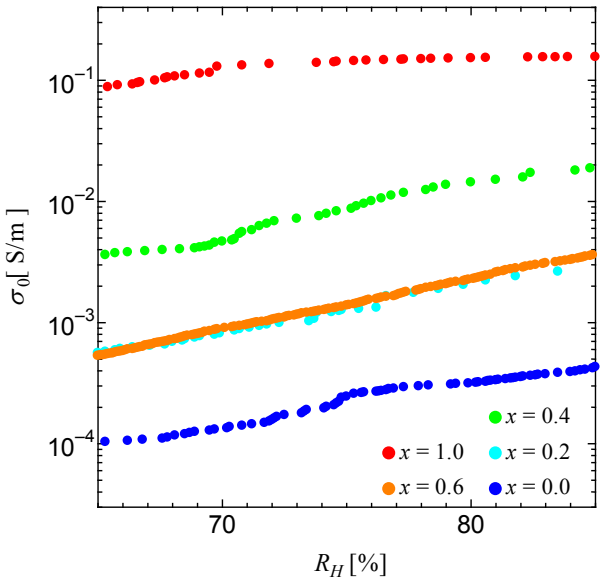

Figure 4. Proton conductivity and relative humidity dependence in chitin-chitosan mixed compounds.

the increase in x. Thus, considering that the mixing ratio x dependence of σ_0 shows the anomalous behavior, x contains an important factor in determining proton conductivity.

In order to examine the mixing ratio x and proton conductivity in detail, the relation between x and σ_0 at the 80% relative humidity is plotted in **Figure 5**. As shown in **Figure 5**, it was found that there is an anomalous correlation between x and σ_0 and that a large peak around $x = 0.75$ and a small peak around $x = 0.4$ are observed. It has been already clarified that the difference of proton conductivity between chitin and chitosan is mainly caused by the presence of the acetyl group. In the case of chitin, high-proton conductivity is realized by the water network formed between the fibers. On the other hand, chitosan, which is a deacetylated form of chitin, forms strong hydrogen bonds between chitosan-main chains due to the amino group exposed by the deacetylation, and the hydration number decreases and therefore proton conductivity decreases. Considering these facts, it seems that the increase in chitosan content, that is, the decrease in x, leads to a monotonous decrease in proton conductivity. However, the measured result shows the two peaks around $x = 0.4$ and 0.75. This result is very interesting, because we can control proton conductivity by adjusting the amount of acetyl-group (that is, the amount of x) and will be helpful to understand the main factor for the appearance of proton conductivity in chitin-type polymer.

In order to understand this anomalous behavior of proton conductivity, we have investigated the change of hydration for the mixing ratio using IR spectra. **Figure 6** shows IR spectra in the samples with various mixing ratios of chitin and chitosan. Here, IR spectra of dry and wet conditions are shown in **Figure 6(a)** and **Figure 6(b)**, respectively. In these figures, IR spectra are normalized by

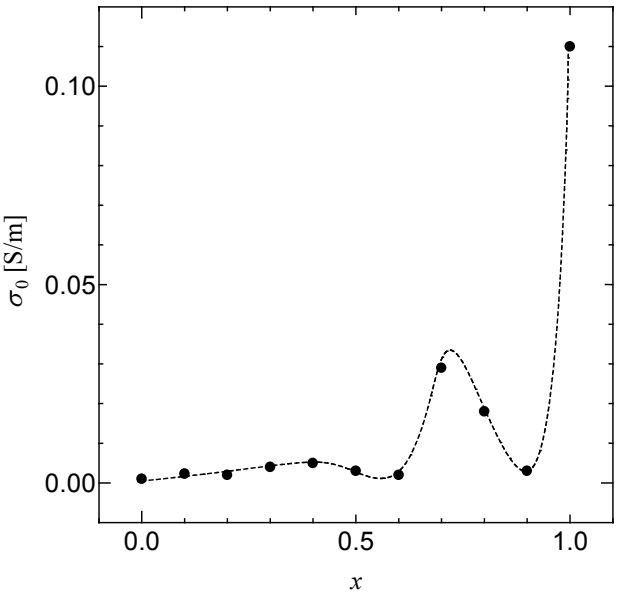

Figure 5. Relationship between DC proton conductivity σ_0 and mixing ratio x at 80% relative humidity. The dotted line is the guide to eyes.

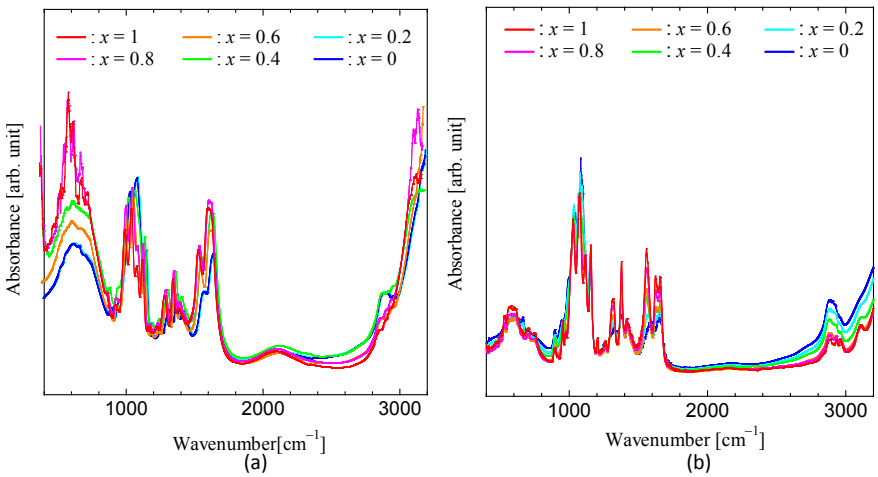

Figure 6. IR spectrum in samples with mixing ratio of various x. (a) dry condition and (b) wet condition. Red and blue lines show chitin (x = 1) and chitosan (x = 0). Other lines, pink, orange green and sky blue show x = 0.8, 0.6, 0.4 and 0.2, respectively.

the absorbance of C-O stretching (1070 cm^{-1}) at which no change between chitin and chitosan is observed in the IR spectrum. As shown in **Figure 6**, the IR spectra remarkably changes by water content and the drastic spectrum changes due to the existence of water are observed in the wet sample. As shown in **Figure 6(a)**, it can be seen that the peak appearing in the vicinity of 1600 cm^{-1} increases as the mixing ratio x = 0 increases to x = 1. It is known that the absorption band appearing near 1600 cm^{-1} is the absorption of Amide I derived from the amino acetyl group of chitin. Therefore, the results in **Figure 6(a)** show that the mixing ratio and the absorbance peak at 1600 cm^{-1} in the dried sample are consistent. Comparing **Figure 6(a)** and **Figure 6(b)**, the wet sample shows large change in

peak at around 600 cm^{-1} and 1600 cm^{-1}, and above 3000 cm^{-1}. It was also found that there was a peak that appeared only in the wet sample even at 2100 to 2200 cm^{-1}. These results indicate that the difference between wet and dry samples is due to the presence or absence of water molecule. In order to make clear the effect of hydration, it is necessary to extract only the absorbance of water molecule without the overlapping with other spectra. It is known that there are several absorption bands of chitin and chitosan around 650 - 690 cm^{-1} (OH out of plane), 1630 - 1660 cm^{-1} (Amide I band) and 3100 - 3450 cm^{-1} (NH and OH stretching), and therefore it is difficult to extract only the effect of water molecule using the IR spectra around these bands [14] [15] [16]. It is also known that IR spectrum around 2110 cm^{-1} remarkably changes by hydration and that doesn't overlap with other peaks [17] [18] [19] [20]. Therefore, in the present work, the effect of hydration is extracted using the difference spectra at the peak around 2110 cm^{-1}.

Figure 7 shows relationship between absorption intensity and the mixing ratio x. Here, the absorption intensity is calculated by the integration of the difference between dry and wet spectra around 2110 cm^{-1}. As shown in Figure 7, it is evident that the change in the intensity of the peak is not monotonous change but the abnormal behavior with the change in the mixing ratio x. The absorption intensity of chitin ($x = 1$) is the strongest, and the peaks of absorption intensity are observed around $x = 0.75$ and 0.4. It is noted that as shown in Figure 5 proton conductivity also shows the peaks around $x = 0.75$ and 0.4. In this way, the anomalous behavior of proton conductivity in Figure 5 is closely related to that of the absorption intensity corresponding to the effect of water. Considering that the absorption intensity is determined by the number of water content, the anomalous behavior of proton conductivity in Figure 5 is caused by the amount

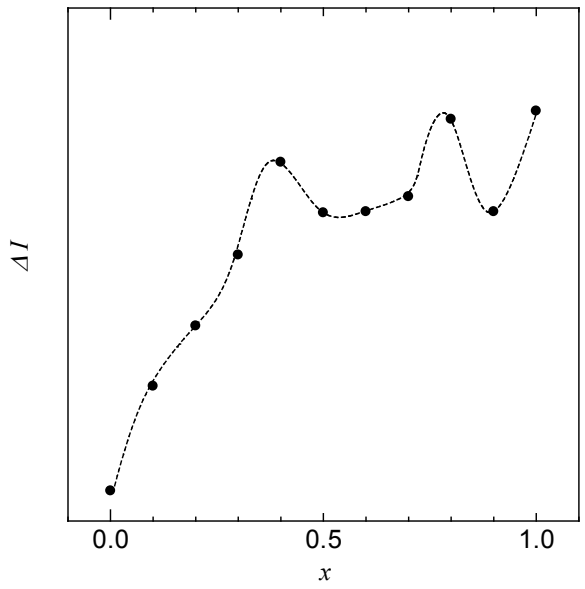

Figure 7. Relationship between peak intensity and mixing ratio x. The dotted line is the guide to eyes.

of water molecule included in chitin-chitosan mixed compounds. That is, the main factor determining proton conductivity in chitin-chitosan mixed compounds is the amount of water content. Therefore, these results indicate that we can control proton conductivity in the chitin-type polymer by adjusting the amount of water content. These results can be used to produce the conducting film with various proton conductivities and can be applied to the fabrication of fuel-cell electrolyte or electrical devices. The challenges to these applications will appear in other articles. In addition, it is known that the number of hydrogen bonds between water molecules and the side chain in chitin is many in comparison with that in chitosan. On the other hand, the space, where water molecule is bonded with the side chain of chitin or chitosan will be expanded by deacetylation. Considering these facts, the anomalous behavior of water contents in **Figure 7** may be caused by the water contents determined by the balances between the amount of the side chain-water molecule hydrogen bond and the number of the space where waters bind with the chitin or chitosan molecule. We are now planning to measure the structure of hydrated chitin-chitosan mixed compounds using the X-ray and neutron diffraction measurements, in order to understand the hydration process in the chitin-chitosan mixed compounds. These results will appear in next issue.

4. Conclusion

In order to investigate the main factor of proton conductivity in chitin-chitosan mixed compounds, the mixed membranes of $(\text{chitin})_x(\text{chitosan})_{1-x}$ were prepared and proton conductivity was investigated. Proton conductivity in the chitin-chitosan mixed compounds monotonously increases by increasing relative humidity. These results indicate that the humidified condition is important for the realization of proton conductivity in chitin-type polymers. Moreover, proton conductivity in chitin is approximately 10^3 times higher than that in chitosan. From these results, it seems that proton conductivity monotonously decreases by decreasing x in $(\text{chitin})_x(\text{chitosan})_{1-x}$. However, we can obtain that the mixing ratio x dependence of proton conductivity has two peaks around $x = 0.75$ and $x = 0.4$. That is, proton conductivity has optimal conditions for the realization of high-proton conductivity in $(\text{chitin})_x(\text{chitosan})_{1-x}$. This result is very interesting and allows us to control proton conductivity by adjusting the number of acetyl-group. Furthermore, in order to investigate the cause of the anomalous behavior for the x dependence of proton conductivity, we have measured FT-IR spectra in dry and wet $(\text{chitin})_x(\text{chitosan})_{1-x}$ specimens. From these results, it was clarified that the absorption intensity around 2110 cm^{-1}, where the intensity remarkably changes by the amount of water content, has peaks around $x = 0.75$ and 0.4. These values are in good agreement with the values of x, where proton conductivity has peaks as shown in **Figure 5**. From these results, it was found that proton conductivity in $(\text{chitin})_x(\text{chitosan})_{1-x}$ is determined by the amount of water content changed by x. In addition, using these results, we can control pro-

ton conductivity in the chitin-type polymer by adjusting the amount of the mixing ratio *x*, and will be able to apply to the fabrication of the conducting film such as fuel-cell electrolytes or thin film transistors.

Acknowledgements

We would like to appreciate Prof. Hiroshi Matsui in Tohoku University for useful discussion on FT-IR measurements. This work was partially supported by JSPS KAKENHI Grant Number 18K11741.

Conflicts of Interest

The authors declare no conflict of interest.

References

[1] Dutta, P.K., Dutta, J. and Tripathi, V.S. (2004) Chitin and Chitosan: Chemistry, Properties and Applications. *Journal of Scientific and Industrial Research*, **63**, 20-31.

[2] Narayan, R.J. (2010) The Next Generation of Biomaterial Development. *Philosophical Transactions of the Royal Society A*, **368**, 1831-1837. https://doi.org/10.1098/rsta.2010.0001

[3] Suginta, W., Khunkaewla, P. and Schulte, A. (2013) Electrochemical Biosensor Applications of Polysaccharide Chitin and Chitosan. *Chemical Reviews*, **113**, 5458-5479. https://doi.org/10.1021/cr300325r

[4] Allan, G., Crospy, G.D., Lee, J.H., Miller, M.L. and Reif, W.M. (1972) New Bonding Systems for Paper. *Man-Made Polymers Paper Making*, Helsinki, 85.

[5] Nair, K.G.R. and Madhavan, P. (1984) Utilization of Prawn Waste—Isolation of Chitin and Its Conversion to Chitosan. *Fishery Technology*, **21**, 109.

[6] Schwarz, S., Steinbach, C., Schwarz, D., Mende, M. and Boldt, R. (2016) Chitosan—The Application of a Natural Polymer against Iron Hydroxide Deposition. *American Journal of Analytical Chemistry*, **7**, 623-632. https://doi.org/10.4236/ajac.2016.78058

[7] Balassa, L.L. (1971) Blooming Grove. Pat. No. 3903268, New York.

[8] Nunthanid, J., Luangtana-anan, M., Sriamornsak, P., Limmatvapirat, S., Huanbutta, K. and Puttipipatkhachorn, S. (2009) Use of Spray-Dried Chitosan Acetate and Ethylcellulose as Compression Coats for Colonic Drug Delivery: Effect of Swelling on Triggering *in Vitro* Drug Release. *European Journal of Pharmaceutics and Biopharmaceutics*, **71**, 356. https://doi.org/10.1016/j.ejpb.2008.08.002

[9] Tripathi, S., Mehrotra, G.K. and Dutta, P.K. (2011) Chitosan-Silver Oxide Nanocomposite Film: Preparation and Antimicrobial Activity. *Bulletin of Materials Science*, **34**, 29-35. https://doi.org/10.1007/s12034-011-0032-5

[10] Kim, E., Xiong, Y., Cheng, Y., Wu, H., Liu, Y., Morrow, B.H., Ben-Yoav, H., Ghodssi, R., Rubloff, G.W., Shen, J., Bentley, W.E., Shi, X. and Payne, G.F. (2015) Chitosan to Connect Biology to Electronics: Fabricating the Bio-Device Interface and Communicating across This Interface. *Journal of Polymer*, **7**, 1-46. https://doi.org/10.3390/polym7010001

[11] Kenawy, E.I.-R.S., Azaam, M.M. and Saad-Allah, K.M. (2015) Synthesis and Antimicrobial Activity of α-Aminophosphonates Containing Chitosan Moiety. *Arabian Journal of Chemistry*, **8**, 427-432. https://doi.org/10.1016/j.arabjc.2013.12.029

[12] Kawabata, T. and Matsuo, Y. (2018) Chitin Based Fuel Cell and Its Proton Conductivity. *Materials Sciences and Applications*, **9**, 779-789. https://doi.org/10.4236/msa.2018.910056

[13] Kawabata, T. and Matsuo, Y. (2019) Aniisotropic Proton Conductvity in Chitin System. *J Mater*, **5**, 258.

[14] Barwin, A., Ramasamy, P., Vairamani, S. and Shanmugam, A. (2011) Physicochemical Characterization of Biopolymers Chitin and Chitosan Extracted from Squid Doryteuthis Sibogae Adam, 1954 PEN. *International Journal of Pharmaceutical Research and Development*, **2**, 18.

[15] Zvezdova, D. (2010) Synthesis and Characterization of Chitosan from Marine Sources in Black Sea. *Annual Proceedings/Association for the Advancement of Automotive Medicine*, Vol. 49, 65-69.

[16] Kameoka, T., Okuda, T., Hashimoto, A., Noro, A., Shinoki, Y. and Ito, K. (1998) FT-IR Analysis of Sugars in Aqueous Solution Using ATR Method. *Nippon Shokuhin Kagaku Kaishi*, **45**, 192. https://doi.org/10.3136/nskkk.45.192

[17] Bertie, J.E. and Whalley, E. (1964) Infrared Spectra of Ices Ih and Ic in the Range 4000 to 350 cm^{-1}. *The Journal of Chemical Physics*, **40**, 1637. https://doi.org/10.1063/1.1725373

[18] Zimmermann, R. and Pimentel, G.C. (1962) In: Mangini, A., Ed., *Advances in Molecular Spectroscopy*, Macmillan, New York, Vol. 2, 726.

[19] Schwarz, H.A. (1977) Gas Phase Infrared Spectra of Oxonium Hydrate Ions from 2 to 5 μ. *The Journal of Chemical Physics*, **67**, 5525-5534. https://doi.org/10.1063/1.434748

[20] Okumura, M., Yeh, L.I., Myers, J.D. and Lee, Y.T. (1990) Infrared Spectra of the Solvated Hydronium Ion: Vibrational Predissociation Spectroscopy of Mass-Selected H_3O^+.cntdot.(H_2O)n.cntdot.(H_2)m. *The Journal of Chemical Physics*, **94**, 3416-3427. https://doi.org/10.1021/j100372a014